Article

Enantioseparation of *syn*- and *anti*-3,5-Disubstituted Hydantoins by HPLC and SFC on Immobilized Polysaccharides-Based Chiral Stationary Phases

Mladenka Jurin [ID], **Darko Kontrec *, Tonko Dražić** [ID] **and Marin Roje**

Department of Organic Chemistry and Biochemistry, Ruđer Bošković Institute, Bijenička cesta 54, 10 000 Zagreb, Croatia; mladenka.jurin@irb.hr (M.J.); tdrazic@gmail.com (T.D.); marin.roje@irb.hr (M.R.)
* Correspondence: darko.kontrec@irb.hr

Abstract: The enantioseparation of *syn*- and *anti*-3,5-disubstituted hydantoins **5a–i** was investigated on three immobilized polysaccharide-based columns (CHIRAL ART Amylose-SA, CHIRAL ART Cellulose-SB, CHIRAL ART Cellulose-SC) by high performance liquid chromatography (HPLC) using *n*-hexane/2-PrOH (90/10, *v*/*v*) or 100% dimethyl carbonate (DMC) as mobile phases, respectively, and by supercritical fluid chromatography (SFC) using CO_2/alcohol (MeOH, EtOH, 2-PrOH; 80/20, *v*/*v*) as a mobile phase. The chromatographic parameters, such as separation and resolution factors, have indicated that Amylose-SA is more suitable for enantioseparation of the most analyzed *syn*- and *anti*-3,5-disubstituted hydantoins than Celullose-SB and Cellulose-SC in both HPLC and SFC modalities. All three tested columns showed better enantiorecognition ability toward *anti*-hydantoins compared to *syn*-hydantoins, both in HPLC and SFC modes. We have demonstrated that environmentally friendly solvent DMC can be efficiently used as the mobile phase in HPLC mode for enantioseparation of hydantoins on the immobilized polysaccharide-based chiral stationary phases.

Keywords: 3,5-disubstituted hydantoins; HPLC; SFC; enantioseparation; immobilized polysaccharide-based chiral stationary phases; DMC; green solvent

1. Introduction

Imidazolidine-2,4-dione, also well known as hydantoin, is a simple hydantoin five-membered nitrogen heterocyclic compound, with four versatile points of functionalities in its framework. Hydantoins have two nitrogens in position 1 and 3, as well as two carbonyl groups in positions 2 and 4, one of which is between the two nitrogens (Figure 1) [1–3].
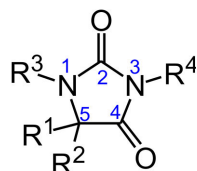
Figure 1. Chemical structure of hydantoins.

The hydantoin moiety is an important structural scaffold present in a number of drugs or drug candidates [3–5]. Phenytoin, ethotoine and norantoine are marketed as anticonvulsant drugs; nilutamide is a nonsteroidal androgen receptor antagonist for the treatment of metastatic prostate cancer [6,7], and BMS-564929 is an orally active and nonsteroidal tissue selective androgen receptor modulator [8]. In addition, hydantoins demonstrate numerous other interesting pharmacological activities, such as antibacterial [9], antiviral [10–13], antifungal [14], antiarrhythmic [15–17], antidiabetic [18,19], antitumor [20–23], antithrombotic, anti-inflammatory and antitussive [24], as well as inhibitory activity against some enzymes

(human aldose reductase and leucocyte elastase) [25,26]. Finally, some herbicides [27–30], fungicides and insecticides also have a hydantoin ring in their structure [29,30].

The hydantoin ring also constitutes the core structure of various natural products, mostly isolated from different marine organisms, but also from bacteria [31]. For example, hemimycallins A and B were isolated from marine sponge *Hemimycale arabica* [26], mukanadine B was isolated from marine sponge *Agelas nakamurai* [32], midpacamide from Fidijan sponge *Agelas mauritiana* [33], and parazoanthines A-J from the Mediterranean Sea anemone *Parazoanthus axinellae* [34,35].

The enantiomers of eighteen chiral 3,5-disubstituted hydantoins were separated by Kartozia et al. using HPLC under normal phase mode on three polysaccharide columns Chiralpak AD-H, Chiralcel OD-H and Chiralcel OJ-H. In this study, a separation of seventeen out of eighteen chiral hydantoins achieved partial or baseline separation on Chiralpak AD-H. For most hydantoins, better separations were obtained on Chiralcel OD-H than on Chiralcel OJ-H [5]. More recently, the enantioseparation of eleven 3,5-disubstituted hydantoins was investigated by Yang et al. using HPLC under the normal phase mode on Chiralpak IA. In the study, the effect of polar alcoholic modifier, ethanol (EtOH), 1-propanol, 2-propanol (2-PrOH), 1-butanol and *tert*-butanol; and column temperature on retention and enantioseparation was evaluated. Additionally, two kinds of enantiomer elution order (EEO) reversals, which include solvent-induced EEO reversal for one tested chiral hydantoin and temperature-induced EEO reversals for the two hydantoins were found [3].

The chiral stationary phases (CSPs) most commonly used are based on silica coated with chiral polysaccharide derivatives, *tris*(carbamates) or *tris*(esters) of amylose or cellulose [36]. These coated CSPs are able to resolve a large variety of structurally different compounds [37,38] and are widely used in HPLC and SFC [39]. These CSPs can only be used with a limited range of solvents as mobile phases such as hydrocarbons, alcohols, acetonitrile (ACN), or hydrocarbon/alcohol and ACN/alcohols mixtures [40]. The immobilized CSPs were prepared by covalently bonding polysaccharide derivates to silica surface [36]. The immobilization allows the use of solvents that cannot be applied on the coated CSPs, such as ethers, esters, ketones and chlorinated hydrocarbons [40]. The enantiorecognition ability of polysaccharide-based CSPs depends on the interactions between the analyte enantiomers and polar carbamate moiety of the polysaccharide-based selector. Each enantiomer forms short-lived, transient diastereomeric complexes with the chiral selector through interactive forces. The complexes are formed as a result of hydrogen bonding, dipole–dipole interactions, π-π bonding, electrostatic interactions (Van der Waals forces), inclusion complexation and steric effects. The strength of these interactions depends on the structure of the analyte and the chiral selector, and on mobile phase composition [41–43].

Here, we present the use of green solvent dimethyl carbonate (DMC ($CH_3O(C=O)OCH_3$) as a mobile phase in HPLC mode for enantioseparation of chiral 3,5-disubstituted hydantoins **5a–i**. DMC is a nonpolar aprotic solvent, slightly soluble in water (139 g L^{-1}) [44] and miscible with alcohols, esters, ethers, and ketones [45]. It is an environmentally benign [46,47], biodegradable [48], non-corrosive [49] and non-toxic solvent [48]. It can be a potential replacement for methyl ethyl ketone, ethyl acetate, methyl isobutyl ketone, and most of other ketones [50]. Lajin and Goessler introduced DMC as a new organic solvent in HPLC-ICPMS for separation of eleven model compounds, such as theobromine, caffeine, aspirin, acetophenone, dithiodibenzoic acid, toluensulfomide, etc. [51]. They compared the elution behavior of DMC with that of other commonly used organic solvents, such as methanol (MeOH), 2-PrOH and acetonitrile. Their results showed that DMC offered stronger elution strength than MeOH and ACN for all tested compounds and stronger elution strength than 2-PrOH for most tested compounds.

In the present work, we have studied the enantioseparation of eighteen chiral 3,5-disubstituted hydantoins **5a–i** (Figure 2) by HPLC under normal standard and non-standard mobile phases. We have also studied the enantioseparation of these hydantoins by SFC using a mobile phase consisting of supercritical carbon dioxide and alcohol (80/20, *v/v*). Three CSPs in their immobilized form (CHIRAL ART Amylose-SA, CHIRAL ART

Cellulose-SB, CHIRAL ART Cellulose-SC) were employed to explore their enantioselectivity. Each analyzed hydantoin possessed two centers of chirality, one in the hydantoin ring and the other in the side chain (Figure 3).
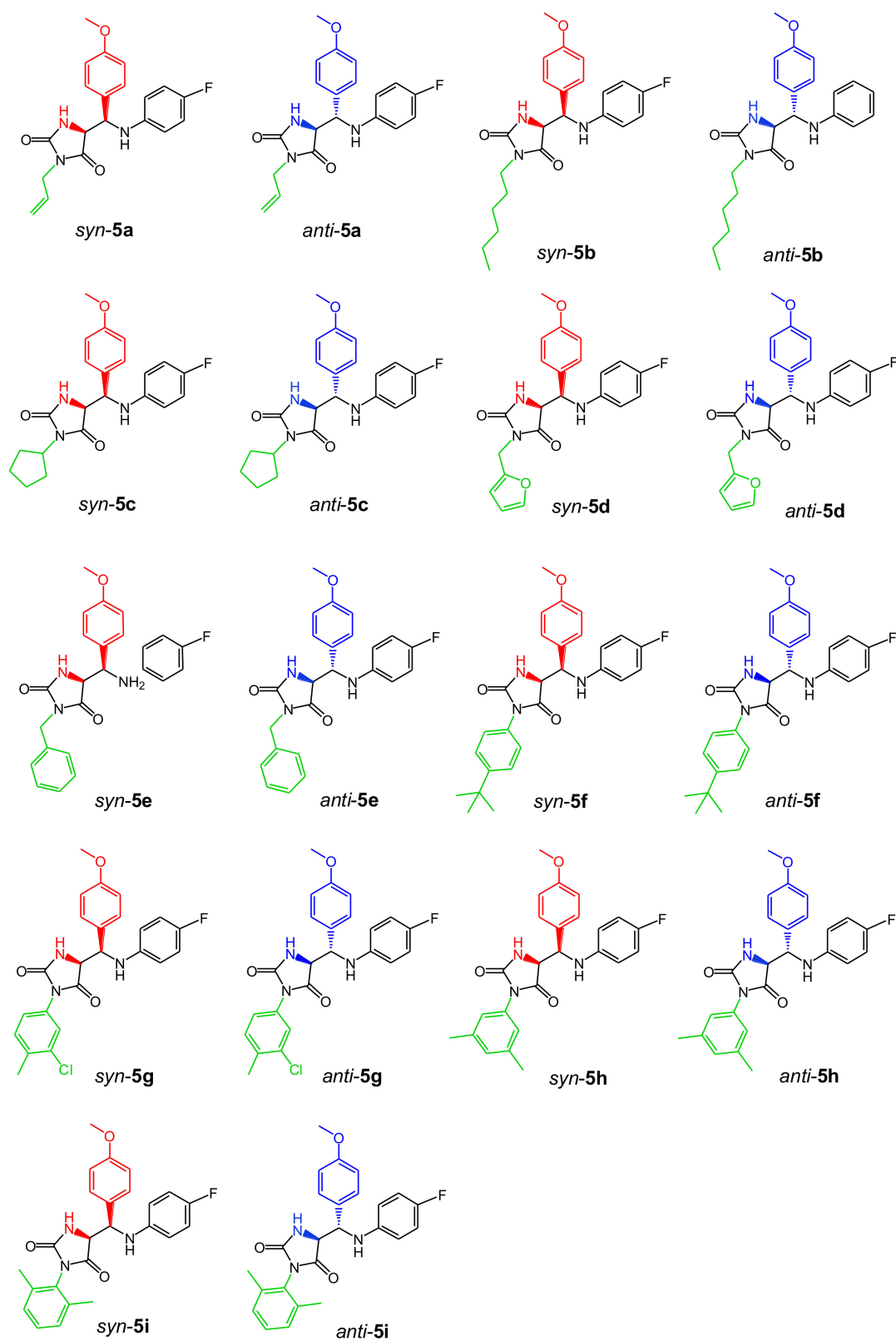

Figure 2. Chemical structures of (±)-*syn*- and (±)-*anti*-3,5-disubstituted hydantoins **5a–i**.
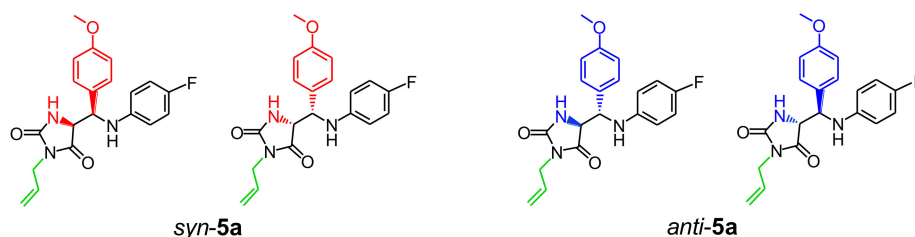
Figure 3. All four possible stereoisomers of allylhydantoin **5a**.

2. Materials and Methods

All used chemicals were purchased from commercial suppliers Sigma Aldrich (Steinheim, Germany), Merck (Darmstadt, Germany) and Fluka (Buchs, Switzerland). Dichloromethane (DCM), EtOH and ACN were dried prior to use according to standard methods [52]. EtOH, MeOH, 2-PrOH and *n*-hexane of HPLC grade were purchased from Honeywell (Seelze, Germany). DMC was purchased from Acros Organics (Geel, Belgium). Liquid CO_2 (grade 4.5) was from Messer (Zagreb, Croatia). The immobilized polysaccharide-based CSPs: CHIRAL ART Amylose-SA S-10 μm, CHIRAL ART Cellulose-SB S-10 μm and CHIRAL ART Cellulose-SC S-10 μm were purchased as bulk material from YMC (Kyoto, Japan). The empty stainless-steel HPLC columns, dimensions 250 mm × 4.6 mm ID, were purchased from Knauer GmbH (Berlin, Germany), and packed with the above mentioned CSPs.

The hydantoins used in this study were synthesized based on a procedure previously described in the literature, Scheme 1. β-Lactam ureas were prepared in four steps via Staudinger reaction [53]. Briefly, the first step included preparation of imine **1** by a condensation reaction of 4-methoxybenzaldehyde and 4-fluoroaniline in dry DCM. In a second reaction, imine **1** was treated with *N*-phthaloylglycine in the presence of triethylamine and 2-chloro-1-methylpyridinium iodide to afford a *cis/trans*-(±)-3-phthalimodo-β-lactam **2**. The *cis*:*trans* ratio was 1:5. In the subsequent step, deprotection of the bulky phthalimide group in the compound *trans*-**2** with ethylenediamine in dry EtOH afforded a free amine, (±)-*trans*-3-amino-β-lactam **3** [54]. The treatment of (±)-*trans*-3-amino-β-lactam **3** with various aliphatic and aromatic isocyanates in dry ACN at room temperature resulted in the isolation of (±)-*trans*-β-lactam ureas **4a–i** [55]. Diastereomeric mixtures (*syn*- and *anti*-) of racemic 3,5-disubstituted hydantoins **5a–i** were synthesized via base-promoted intramolecular amidolysis of (±)-*trans*-β-lactam ureas **4a–i** [56]. The mixtures of diastereomeric hydantoins were then separated by preparative RP-HPLC using preparative column Zorbax Extend-C18 PrepHT (250 × 9.4 mm I.D., 5-μm particle size, 300 Å pore size) from Agilent Technologies (Waldbronn, Germany) with a linear gradient AB at a flow rate of 17 mL min^{-1}, where mobile phase A was water and mobile phase B was ACN. The structures of all *syn*- and *anti*-hydantoins **5a–i** are shown in Figure 2. All compounds were characterized by NMR, IR and mass spectroscopy.

Two chromatographic systems were applied in this study. The first one was an Agilent 1200 Series HPLC System (Agilent Technologies, Waldbronn, Germany), equipped with a vacuum degasser, a quaternary pump, a thermostated column compartment, an autosampler and a variable wavelength detector. The mobile phase was *n*-hexane/2-PrOH (90/10, *v/v*) or 100% DMC. All experiments in normal-phase mode and non-standard mode were carried out under isocratic conditions at a flow rate of 1.0 mL min^{-1} and at a column temperature of 30 °C. The injection volume was 20 μL. Data analysis and processing were carried out by EZChrom Elite software version 3.1.7. (Agilent Technologies, Waldbronn, Germany).
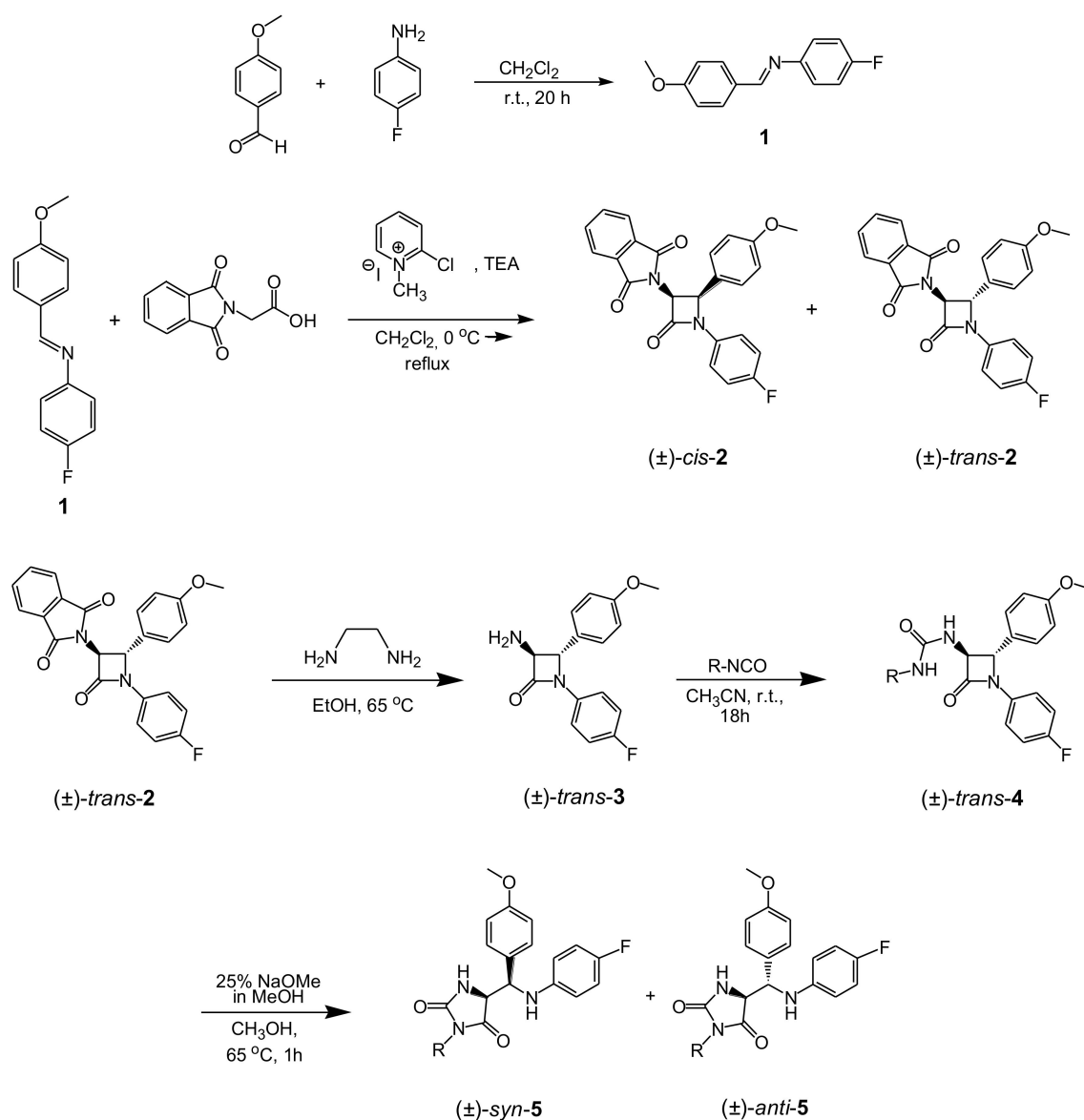
Scheme 1. Synthesis of (±)-*syn*- and (±)-*anti*-3,5-disubstituted hydantoins **5**.

The second chromatographic system, an Agilent 1260 Infinity II Hybrid SFC/UHPLC (Agilent Technologies, Waldbronn, Germany) system, was applied for SFC studies. It consisted of an Infinity SFC binary pump, an Aurora A5 Fusion module, a degasser, an autosampler, a thermostated column compartment, a diode array detector and a backpressure regulator. The system was controlled by Open LAB CDS ChemStation Edition Rev. C01.08 software (Agilent Technologies, Waldbronn, Germany). In every case, SFC was performed in isocratic mode at a flow rate of 4.0 mL min^{-1} and a column temperature of 35 °C. The injection volume was 20 µL and the outlet pressure was set at 15 MPa. The mobile phases applied in SFC consisted of CO_2 and MeOH, EtOH or 2-PrOH, each in the ratio 80/20, *v/v*. Detection was performed at a wavelength of 254 nm using a diode-array detector.

Sample solutions of the analytes were prepared by dissolving hydantoin compounds in *n*-hexane/2-PrOH (90/10, *v/v*), DMC or MeOH in 0.5 mg mL^{-1} concentration and filtered through RC-45/25 Chromafil® Xtra 0.45 µm syringe filter (Macherey-Nagel GmbH & Co. KG, Düren, Germany). The HPLC columns were packed by using the typical slurry method, where *n*-hexane/2-PrOH (90:10, *v/v*) was used as slurring solvent to prepare *n*-hexane/2-PrOH-YMC bulk materials (CHIRAL ART Amylose-SA, CHIRAL ART Cellulose-SB and CHIRAL ART Cellulose-SC) suspensions with sonication, respectively.

The suspensions were packed into stainless-steel columns (250 × 4.6 mm I.D.) by the conventional high pressure downward slurry technique using a Knauer pneumatic HPLC pump (Knauer Gmbh, Berlin, Germany). In the following text, these columns are marked as Amylose-SA, Cellulose-SB and Cellulose-SC. The chiral selectors in Amylose-SA, Cellulose-SB and Cellulose-SC are amylose *tris*-(3,5-dimethylphenylcarbamate), cellulose *tris*-(3,5-dimethylphenylcarbamate) and cellulose *tris*-(3,5-dichlorophenylcarbamate), respectively; all three are shown in Figure 4.
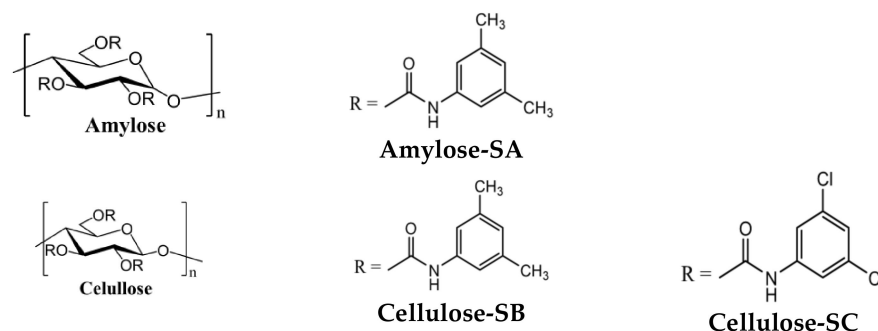

Figure 4. Chemical structures of chiral selectors.

The retention factor of the first and the second eluted enantiomer (k_1 and k_2), the separation factor (α), and the resolution (R_s) are calculated according to the usual formulae:

$$k_1 = (t_{r1} - t_0)/t_0 \tag{1}$$

$$k_2 = (t_{r2} - t_0)/t_0 \tag{2}$$

$$\alpha = k_2/k_1 \tag{3}$$

$$R_s = 2 \times (t_{r2} - t_{r1})/(w_1 + w_2) \tag{4}$$

where t_0 is the dead time, t_{r1} and t_{r2} are the retention times of the first and second eluted enantiomers, respectively, and w_1 and w_2 are the corresponding base peak widths. In HPLC mode, the dead time, which is the retention time of a nonadsorbing component, was determined by injection of 1,3,5-tri-*tert*-butylbenzene, while in SFC mode the first negative signal by injecting MeOH was used.

3. Results and Discussion

The use of DMC in our enantioseparation studies also requested the use of immobilized CSPs. DMC and the other organic solvents of medium polarity (non-standard HPLC solvents), such as acetone, dichloromethane, chloroform, ethyl acetate, methyl *tert*-butyl ether and tetrahydrofuran can be used on immobilized chiral selectors. Contrary, these solvents cannot be used with coated polysaccharide-based chiral selectors, because they can dissolve or swell the polysaccharide derivative [57–59]. In this study, our intention was to demonstrate an efficient replacement of hydrocarbon-based mobile phase with DMC and/or supercritical CO_2.

3.1. Enantioseparation on Amylose-SA

The results of the HPLC and SFC enantioseparation using Amylose-SA column are summarized in Table 1. The Amylose-SA allowed the enantioseparation of all eighteen analyzed 3,5-disubstituted hydantoins under the *n*-hexane/2-PrOH (90/10, *v/v*) mobile phase system. Among them, for seventeen pairs of enantiomers the baseline separation was achieved, while partial separation was observed only for the enantiomers of the compound *syn*-**5i**. In the normal phase mode, the retention factors (k_1) of the first eluting enantiomers of the *syn*- and *anti*-compounds **5h** and **5i** were higher than that of other hydantoins, which implied that the interactions between these analytes and CSP were the strongest. The possible reason may be the presence of two methyl groups at either *ortho*- or *meta*-position

of the N3 phenyl ring in **5h** and **5i**, respectively. On the contrary, the lower retention of compounds *syn*-**5b**, *anti*-**5b**, *syn*-**5c** and *anti*-**5c** was the result of their weaker interaction with CSP. The possible reason may be the presence of alkyl or cycloalkyl substituent at the N3 position of the hydantoin ring, which, unlike other tested hydantoins, cannot provide additional π-π interactions with the CSP. It is obvious that the longer retained compounds did not always accomplish higher separation factors and resolution. Moreover, this column exhibited better chiral recognition toward *anti*-hydantoins **5a–i** compared to *syn*-hydantoins **5a–i**. When DMC was used as the mobile phase, among eighteen hydantoins, a baseline separation was achieved for eight hydantoins while six hydantoins were partially separated. The enantiomers of the hydantoins *syn*-**5a**, *syn*-**5d**, *anti*-**5c**, and *anti*-**5f** did not separate on this column under the same condition. As seen from Table 1, better enantioselectivity of compounds *syn*-**5b**, *syn*-**5f**, *syn*-**5g**, *syn*-**5i** was achieved with DMC as the mobile phase, while the resolution was always higher with *n*-hexane/2-PrOH (90/10, *v/v*) as the mobile phase. Moreover, under DMC conditions, *anti*-hydantoins **5a**, **5b**, **5d**, **5e**, **5h** and **5i** showed higher α and R_s values compared to α and R_s of their *syn*-isomers. *syn*-Hydantoins **5c** and **5f** showed better results (in terms of α and R_s) than *anti*-**5c** and *anti*-**5f**; the *syn*-isomers were partially separated, while *anti*-isomers were not resolved under DMC. Furthermore, the enantiomers of compound *anti*-**5g** achieved greater resolution and lower value of separation factor compared to the enantiomers of compound *syn*-**5g** under non-standard mobile phase. DMC as the hydrogen bond acceptor is capable of interacting with the polarized hydrogen atom of the carbamate N-H group (hydrogen bond donor) of amylose-based selector, competing with hydantoin compounds for hydrogen bonding sites, therefore accelerating the elution rate. As shown in Figure 5, *syn*-allyl hydantoin **5a** expressed a superior R_s of 3.23 and α of 1.61 on Amylose-SA under *n*-hexane/2-PrOH (90/10, *v/v*) compared to R_s 0 and α of 1.44 under 100% DMC. *anti*-Allyl hydantoin **5a** showed R_s of 6.36 and α of 2.48 under *n*-hexane/2-PrOH (90/10, *v/v*) compared to R_s of 1.57 and α of 2.25 under 100% DMC. In particular, Amylose-SA showed a significantly higher resolution and enantioselectivity values for the *anti*-allyl hydantoin **5a** under the normal and non-standard HPLC conditions.

Table 1. Chromatographic parameters for the enantioselective separations of racemic *syn*-and *anti*-3,5-disubstituted hydantoins on Amylose-SA.

Compound	Condition *	k_1	k_2	α	R_s	Compound	Condition *	k_1	k_2	α	R_s
syn-**5a**	A	6.57	10.58	1.61	3.23	*anti*-**5a**	A	5.33	13.30	2.48	6.36
	B	0.09	0.09	1.00	-		B	0.16	0.36	2.25	1.57
	C	1.45	1.85	1.28	0.80		C	1.23	2.32	1.89	2.32
	D	1.40	1.78	1.27	0.76		D	1.20	2.15	1.80	2.07
	E	1.34	1.90	1.42	1.21		E	1.34	2.43	1.81	2.23
syn-**5b**	A	2.47	4.51	1.83	3.74	*anti*-**5b**	A	2.04	5.74	2.81	6.27
	B	0.10	0.22	2.20	0.41		B	0.22	0.50	2.27	1.81
	C	1.54	2.19	1.42	1.36		C	1.56	2.76	1.76	2.29
	D	1.39	1.96	1.41	1.21		D	1.32	2.42	1.83	2.28
	E	1.31	2.01	1.53	1.49		E	1.36	2.70	1.99	2.55
syn-**5c**	A	2.85	5.30	1.86	3.98	*anti*-**5c**	A	2.85	8.03	2.82	6.43
	B	0.18	0.28	1.56	0.87		B	0.60	0.60	1.00	-
	C	1.34	3.19	2.38	2.90		C	1.70	4.45	2.62	4.60
	D	1.47	2.63	1.79	2.33		D	1.61	3.76	2.34	4.52
	E	1.59	2.63	1.65	1.99		E	1.59	3.93	2.47	3.58

Table 1. *Cont.*

Compound	Condition *	k_1	k_2	α	R_s	Compound	Condition *	k_1	k_2	α	R_s
syn-**5d**	A	6.05	11.63	1.92	4.42	*anti*-**5d**	A	4.95	17.52	3.54	8.63
	B	0.19	0.19	1.00	-		B	0.14	0.30	2.14	1.11
	C	2.08	2.75	1.32	1.12		C	1.78	3.37	1.89	2.72
	D	1.84	2.52	1.37	1.30		D	1.64	3.07	1.87	2.68
	E	1.78	2.82	1.58	1.88		E	1.84	3.99	2.17	3.58
syn-**5e**	A	7.97	16.34	2.05	4.12	*anti*-**5e**	A	4.49	16.01	3.57	8.31
	B	0.17	0.24	1.41	0.54		B	0.28	0.47	1.68	1.38
	C	2.87	3.77	1.31	1.27		C	2.68	4.88	1.82	2.77
	D	2.44	3.57	1.46	1.86		D	2.51	4.33	1.73	3.05
	E	2.39	4.16	1.74	2.63		E	2.64	5.76	2.18	3.99
syn-**5f**	A	4.76	8.54	1.79	3.17	*anti*-**5f**	A	3.70	10.04	2.71	4.59
	B	0.14	0.45	3.21	1.97		B	0.32	0.32	1.00	-
	C	3.08	8.34	2.71	4.20		C	3.04	15.51	5.10	7.65
	D	2.91	7.39	2.54	4.03		D	2.82	12.39	4.39	6.56
	E	2.66	6.01	2.26	3.65		E	2.59	9.15	3.53	5.64
syn-**5g**	A	6.85	14.14	2.06	4.30	*anti*-**5g**	A	3.92	10.39	2.65	4.94
	B	0.17	0.61	10.11	3.02		B	0.37	1.72	4.65	5.23
	C	4.63	11.91	2.57	4.46		C	4.25	17.62	4.14	6.20
	D	4.35	10.87	2.50	4.70		D	4.00	15.40	3.85	6.57
	E	3.93	9.39	2.39	4.25		E	3.78	13.00	3.44	5.91
syn-**5h**	A	10.43	21.05	2.02	4.30	*anti*-**5h**	A	6.17	15.89	2.58	4.94
	B	0.15	0.45	3.00	2.19		B	0.25	0.96	3.84	4.55
	C	2.67	5.95	2.23	3.55		C	2.40	7.22	3.01	4.65
	D	2.62	5.90	2.25	3.68		D	2.31	6.86	2.97	4.93
	E	1.91	6.05	3.17	3.02		E	2.39	6.57	2.75	4.57
syn-**5i**	A	14.34	16.13	1.12	0.75	*anti*-**5i**	A	16.81	22.33	1.33	1.77
	B	0.10	0.17	1.70	0.42		B	0.26	0.50	1.92	1.54
	C	2.43	3.30	1.33	1.23		C	2.77	4.25	1.53	1.76
	D	2.81	3.74	1.33	1.34		D	3.41	5.10	1.50	1.83
	E	3.52	5.11	1.45	1.88		E	4.74	8.26	1.74	2.90

* Chromatographic conditions: mobile phase, A, *n*-hexane/2-PrOH (90/10, *v/v*), flow rate 1 mL min^{-1}; B, 100% DMC, flow rate 1 mL min^{-1}; C, CO_2/MeOH (80/20, *v/v*), flow rate 4 mL min^{-1}, backpressure 15 MPa; D, CO_2/EtOH (80/20, *v/v*), 4 mL min^{-1}, backpressure 15 MPa; E, CO_2/2-PrOH (80/20, *v/v*), flow rate 4 mL min^{-1}, backpressure 15 MPa. Detection wavelength for each condition was 254 nm. Column temperature of conditions A and B is 30 °C, of C, D and E is 35 °C. The chromatographic parameters k_1, k_2, α and R_s are defined in Section 2.

Under SFC conditions, we investigated the effect of three modifiers (MeOH, EtOH, 2-PrOH) on enantioseparation of hydantoin derivatives **5a–i**. It is interesting to note that 2-PrOH yields more baseline enantioseparations than MeOH and EtOH, Table 1. By comparing the data obtained with the modifiers MeOH, EtOH or 2-PrOH the retention factors of the first eluted enantiomers of compounds *syn*-**5c**, *syn*-**5i**, *anti*-**5a**, *anti*-**5d** and *anti*-**5i** were the highest with 2-PrOH as the modifier. The retention factors of *syn*-**5c**, *syn*-**5i** and *anti*-**5i** hydantoins increased as the mobile phase modifier changed from MeOH to EtOH and then to 2-PrOH, which should be due to the decrease in solvent polarity and the increase in bulkiness of alcoholic modifiers (due to the chain length and branching). The

compounds *syn*-**5a**, *syn*-**5b**, *syn*-**5d**, *syn*-**5e**, *syn*-**5f**, *syn*-**5g**, *syn*-**5g**, *anti*-**5f**, *anti*-**5g** and *anti*-**5i** followed the opposite trend; the retention factor of the compounds increasing in the order 2-PrOH > EtOH > MeOH. MeOH, EtOH and 2-PrOH are all protic solvents, and they are capable of interacting with amylose *tris*-(3,5-dimethylphenylcarbamate) through hydrogen bonding, and thus compete with the hydantoin compounds for the hydrogen bonding site, thus accelerating the elution rate. When applying a branched-chain alcohol 2-PrOH, it forms weaker hydrogen bonds with CSP than MeOH and EtOH, so the retention factor is expected to be longer. However, it was observed that 2-PrOH gave shorter retention times than straight-chain alcohols (MeOH and EtOH) for ten analyzed compounds *syn*-**5a**, *syn*-**5b**, *syn*-**5d**, *syn*-**5e**, *syn*-**5f**, *syn*-**5g**, *syn*-**5h**, *anti*-**5c**, *anti*-**5f** and *anti*-**5f**. The molecular structure type and the steric effects of the modifiers influence the enantioselectivity and retention of the analyte. The chiral recognition mechanisms of the analytes with Amylose-SA are very complex, and largely depend on the structure of hydantoin derivatives, i.e., the nature of the functional group at the N3 position of the hydantoin ring.
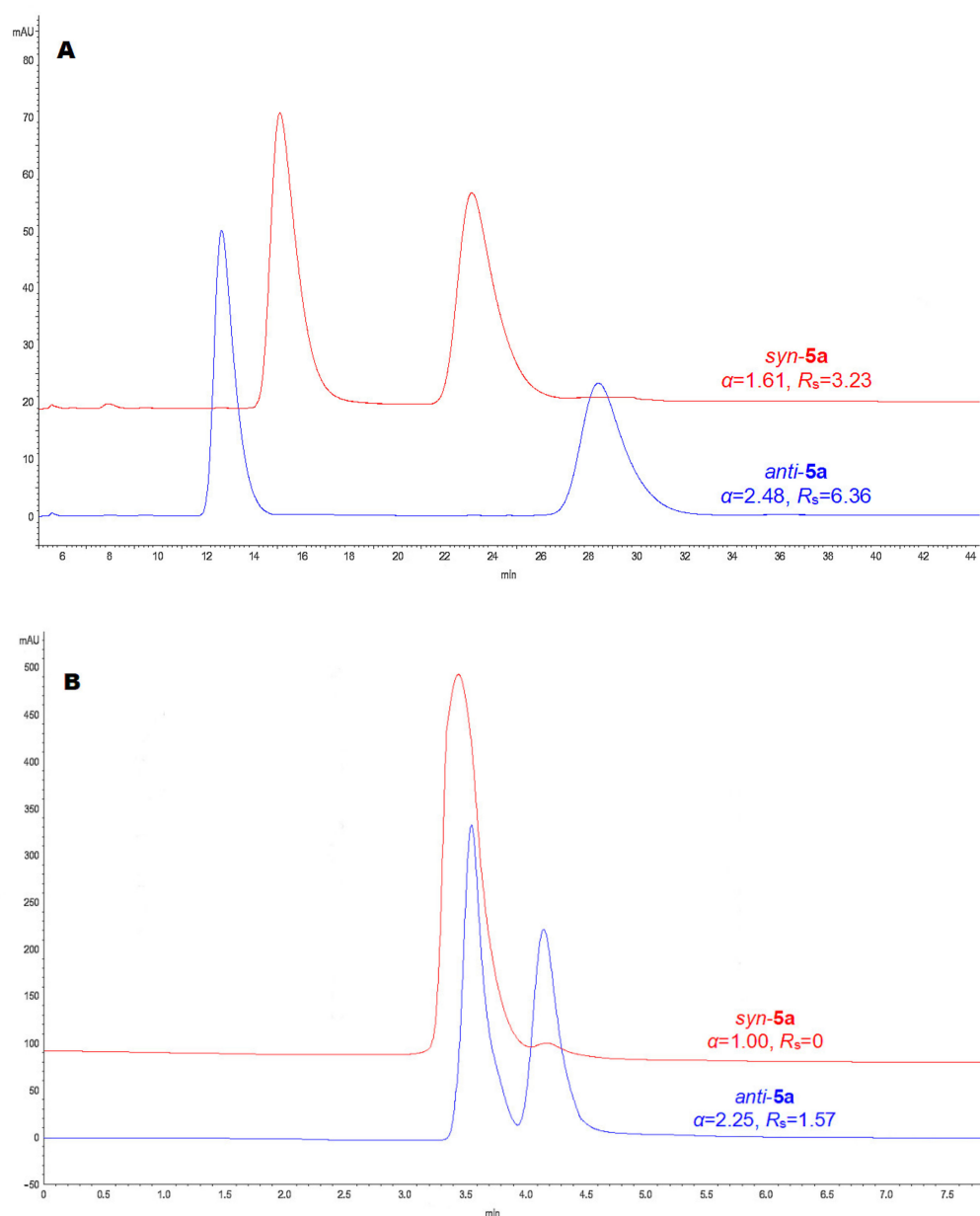

Figure 5. HPLC overlay chromatograms of (±)-*syn*-**5a** and (±)-*anti*-**5a** on Amylose-SA column with: (**A**) *n*-hexane/2-PrOH (90/10, *v/v*) and (**B**) 100% DMC as mobile phases.

The Amylose-SA column under SFC mode exhibits better chiral recognition ability toward *anti*-hydantoins compared to *syn*-hydantoins. As shown in Figure 6, under the mobile phase of CO_2/EtOH (80/20, v/v), both *syn*- and *anti*-allyl hydantoins **5a** have the lowest R_s and α and the largest values for MeOH as the modifier.
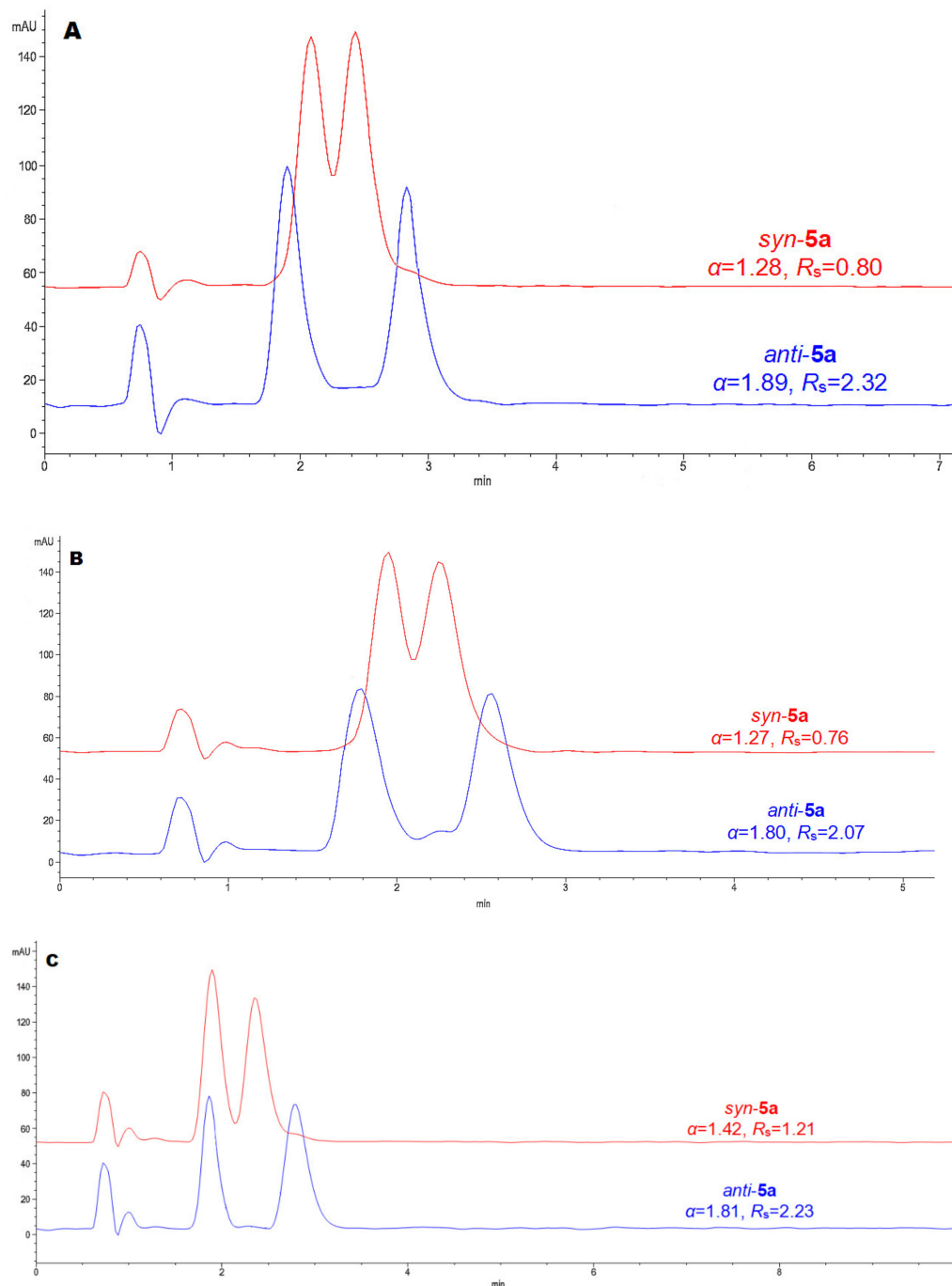

Figure 6. SFC overlay chromatograms of (±)-*syn*-**5a** and (±)-*anti*-**5a** on Amylose-SA column with: (**A**) CO_2/MeOH (80/20, v/v), (**B**) CO_2/EtOH (80/20, v/v) and (**C**) CO_2/2-PrOH(80/20, v/v) as mobile phases.

3.2. Enantioseparation on Cellulose-SB

This CSP contains the same 3,5-dimethylphenylcarbamate substituent as Amylose-SA; however, they differ only in the nature of polysaccharide backbone, i.e., cellulose and amylose. When operating in the normal phase HPLC mode, the Cellulose-SB column

provided a better separation for enantiomers of *anti*-hydantoins **5a–i** compared to *syn*-isomers. It is obvious that the enantiomers of all analyzed *anti*-hydantoins were well separated (R_s > 2.14) on Cellulose-SB along with good enantioselectivity. In contrast to *anti*-hydantoins, seven *syn*-hydantoins were baseline separated on this column while two hydantoins *syn*-**5a** and *syn*-**5c** showed only partial enantioseparation. In general, lower retention and higher α and R_s values were obtained for *anti*-hydantoins **5a–i**. In the normal phase mode, the retention factor of the first eluting enantiomers of the *syn*- and *anti*-compounds **5a** and **5d–i** were always higher than that of other two hydantoins **5b** and **5c**. A possible reason may be the presence of a allyl group (compound **5a**), a furan ring (compound **5d**) or a phenyl ring (compounds **5e–i**) at the N3 position of these hydantoins, which could provide additional π-π interactions between these analytes (donor) and CSP (acceptor). On the other hand, compounds **5b** and **5c** showed the lowest retention under the normal phase mode. This indicates that the interaction between compounds **5b** and **5c** with the stationary phase is weak, possibly due to a hexyl or cycloalkyl substituent at the N3 position of the hydantoin ring, which cannot provide additional interactions with the CSP like other analyzed hydantoins.

When DMC was used as the mobile phase, compounds *anti*-**5a**, *anti*-**5c**, *anti*-**5e** and *anti*-**5i** achieved baseline separation. Among them, compound *anti*-**5i** containing the 2,6-dimethylphenyl group on N3 showed the best separation (R_s = 2.21 and α = 1.90), followed by *anti*-**5c** containing the cyclopentyl moiety on N3 with a *R*s value of 2.15 and α of 2.46. Other *anti*-hydantoins **5b**, **5d**, **5f**, **5g** and **5h** were partially separated. In addition, all nine *syn*-hydantoins **5a–i** were not enantioseparated on this column under the same conditions. It is possible that DMC altered the supramolecular structure of the cellulose chiral selector by modifying the size of the interaction cavity between the polysaccharide chains and made them more suitable for interactions with the *anti*-hydantoins **5a–i**. As seen from Table 2, all analyzed hydantoins were always longer retained in the normal phase than in non-standard phase mode, which indicates that the lower retention of hydantoins was the result of their weaker interaction with CSP. Typical chromatograms of the resolution of the enantiomers of allyl hydantoins *syn*-**5a** and *anti*-**5a** under *n*-hexane/2-PrOH and dimethyl carbamate are shown in Figure 7. It can be seen that the higher retention, and higher separation factor and resolution was obtained for *anti*-**5a** compared to *syn*-**5a** under both HPLC modes.

Table 2. Chromatographic parameters for the enantioselective separations of racemic *syn*-and *anti*-3,5-disubstituted hydantoins on Cellulose-SB.

Compound	Condition *	k_1	k_2	A	R_s	Compound	Condition *	k_1	k_2	α	R_s
	A	13.95	14.93	1.07	0.84		A	7.15	10.38	1.45	4.58
	B	0.12	0.12	1.00	-		B	0.17	0.30	1.76	1.68
syn-**5a**	C	2.91	3.25	1.12	0.71	*anti*-**5a**	C	2.08	3.20	1.54	2.83
	D	2.77	3.05	1.10	0.46		D	1.91	2.62	1.37	1.75
	E	3.71	3.71	1.00	-		E	2.42	3.37	1.39	2.13
	A	8.04	10.33	1.28	3.09		A	4.64	6.36	1.37	3.63
	B	0.12	0.12	1.00	-		B	0.20	0.27	1.35	0.89
syn-**5b**	C	3.07	3.07	1.00	-	*anti*-**5b**	C	2.18	3.20	1.47	2.45
	D	2.82	2.82	1.00	-		D	1.94	2.53	1.30	1.45
	E	3.40	3.80	1.12	0.78		E	2.46	3.18	1.29	1.60

Table 2. *Cont.*

Compound	Condition *	k_1	k_2	A	R_s	Compound	Condition *	k_1	k_2	α	R_s
syn-**5c**	A	7.69	8.63	1.12	1.42	*anti*-**5c**	A	3.47	4.19	1.21	2.14
	B	0.14	0.14	1.00	-		B	0.13	0.32	2.46	2.15
	C	3.46	3.46	1.00	-		C	2.26	2.99	1.32	1.73
	D	3.06	3.06	1.00	-		D	1.93	2.29	1.19	0.98
	E	3.74	3.74	1.00	-		E	2.22	2.66	1.20	1.09
syn-**5d**	A	19.82	23.62	1.19	2.28	*anti*-**5d**	A	11.63	18.08	1.55	5.49
	B	0.09	0.09	1.00	-		B	0.18	0.26	1.44	1.01
	C	4.10	4.60	1.12	0.99		C	3.16	4.77	1.51	3.27
	D	3.90	4.30	1.10	0.73		D	2.86	3.93	1.37	2.33
	E	5.24	5.24	1.00	-		E	3.63	5.22	1.44	2.87
syn-**5e**	A	17.03	22.08	1.30	3.34	*anti*-**5e**	A	11.37	17.44	1.53	5.05
	B	0.11	0.11	1.00	-		B	0.19	0.32	1.68	1.57
	C	5.83	7.02	1.20	1.90		C	5.09	7.94	1.56	4.45
	D	5.27	6.27	1.19	1.65		D	4.32	6.09	1.41	2.98
	E	7.06	7.06	1.00	-		E	5.40	7.67	1.42	3.39
syn-**5f**	A	19.70	34.70	1.76	6.63	*anti*-**5f**	A	10.32	27.59	2.67	10.44
	B	0.11	0.11	1.00	-		B	0.14	0.23	1.64	0.85
	C	5.85	8.78	1.50	3.95		C	4.66	11.98	2.57	5.74
	D	5.43	7.72	1.42	3.37		D	4.43	7.00	1.58	4.23
	E	7.74	9.96	1.29	2.48		E	5.86	9.57	1.63	4.45
syn-**5g**	A	25.61	32.02	1.25	2.97	*anti*-**5g**	A	11.70	23.86	2.04	8.12
	B	0.15	0.15	1.00	-		B	0.22	0.30	1.36	1.08
	C	8.39	10.84	1.29	2.81		C	6.03	10.75	1.78	6.02
	D	7.58	9.39	1.24	2.22		D	5.42	8.12	1.50	3.90
	E	10.73	11.66	1.11	1.09		E	6.98	10.70	1.53	4.34
syn-**5h**	A	21.82	30.92	1.42	4.16	*anti*-**5h**	A	13.66	27.91	2.04	8.32
	B	0.15	0.15	1.00	-		B	0.23	0.33	1.43	0.88
	C	5.96	8.85	1.48	4.01		C	4.17	7.29	1.75	5.15
	D	3.86	5.71	1.48	3.29		D	3.86	5.71	1.48	3.29
	E	7.95	10.00	1.26	2.34		E	4.93	7.99	1.62	4.24
syn-**5i**	A	22.09	31.27	1.42	4.16	*anti*-**5i**	A	8.39	36.14	4.31	13.06
	B	0.13	0.13	1.00	-		B	0.20	0.38	1.90	2.21
	C	6.25	8.43	1.35	3.05		C	4.82	8.51	1.77	5.48
	D	5.87	8.20	1.40	3.26		D	3.91	7.13	1.82	5.35
	E	7.89	11.91	1.51	4.21		E	4.52	10.55	2.33	7.86

* Chromatographic conditions: mobile phase, A, *n*-hexane/2-PrOH (90/10, *v/v*), flow rate 1 mL min^{-1}; B, 100% DMC, flow rate 1 mL min^{-1}; C, CO_2/MeOH (80/20, *v/v*), flow rate 4 mL min^{-1}, backpressure 15 MPa; D, CO_2/EtOH (80/20, *v/v*), 4 mL min^{-1}, backpressure 15 MPa; E, CO_2/2-PrOH (80/20, *v/v*), flow rate 4 mL min^{-1}, backpressure 15 MPa. Detection wavelength for each condition was 254 nm. Column temperature of condition A and B is 30 °C, of C, D and E is 35 °C. The chromatographic parameters k_1, k_2, α and R_s are defined in Section 2.
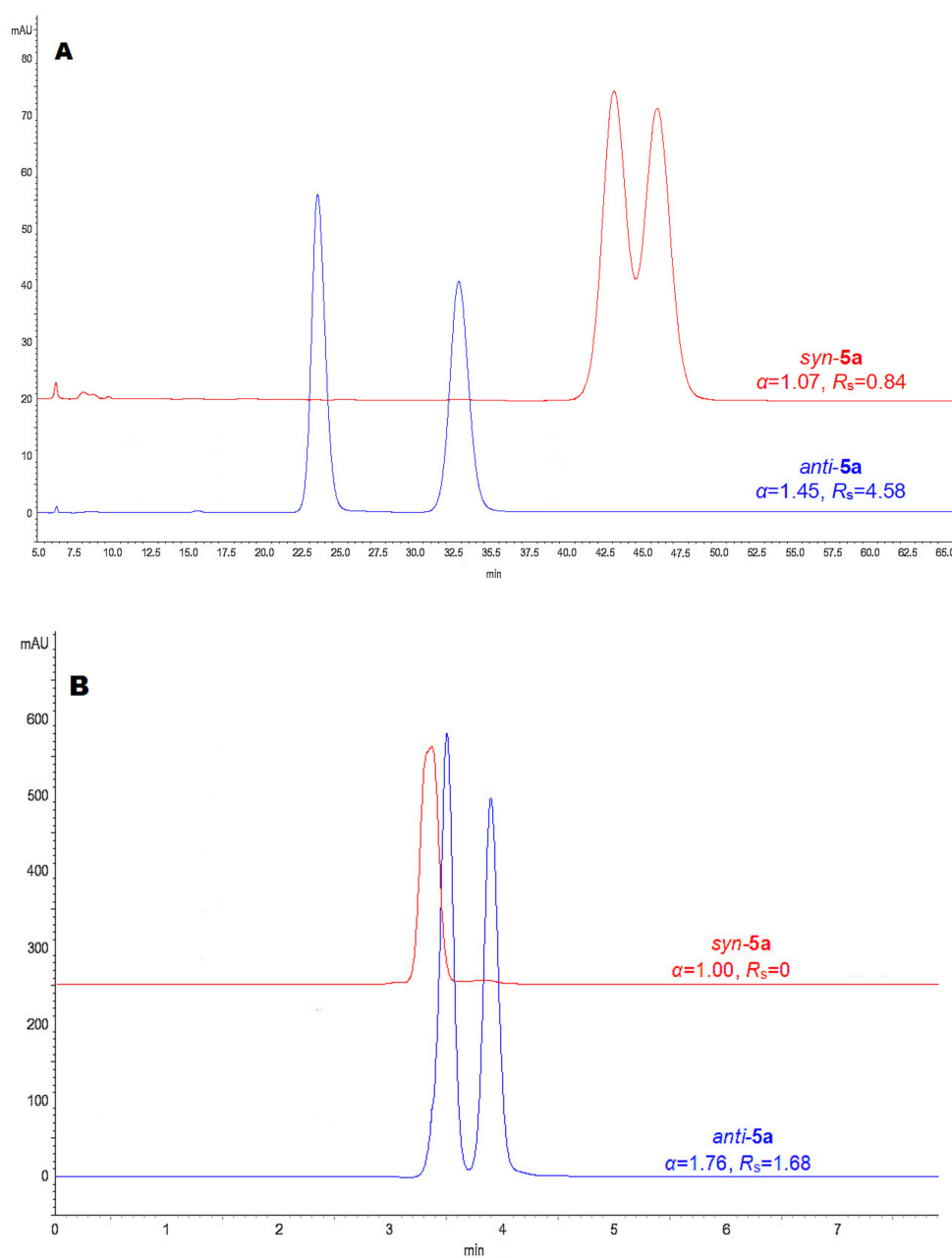
Figure 7. HPLC overlay chromatograms of (±)-*syn*-**5a** and (±)-*anti*-**5a** on Cellulose-SB column with: (**A**) *n*-hexane/2-PrOH (90/10, *v/v*) and (**B**) 100% DMC as mobile phases.

The effects of supercritical carbon dioxide and alcohol modifiers (MeOH, EtOH and 2-PrOH) on the enantioseparation of *syn*- and *anti*-hydantoins are listed in Table 2. From the obtained results, we can notice that compounds *syn*-**5f**, *syn*-**5h**, *syn*-**5i**, *anti*-**5a**, *anti*-**5d**, *anti*-**5e**, *anti*-**5f**, *anti*-**5g**, *anti*-**5h** and *anti*-**5i** were completely separated using all three alcohol modifiers, along with a good resolution. Baseline separation of *syn*-**5e** with benzyl substituent at the N3 position of the hydantoin ring and *syn*-**5g** with 3-chloro-4-methylphenyl substituent at the same position was achieved when MeOH or EtOH were selected as the alcohol modifier; among them, a better separation was obtained with MeOH. Baseline separation of *anti*-**5b** was achieved with MeOH and 2-PrOH, while the baseline separation of *anti*-**5c** was achieved using MeOH, and EtOH compounds *syn*-**5a** and *syn*-**5d** were partially separated using MeOH and EtOH as the polar modifiers. The enantiomers of compound *syn*-**5b** were partially separated on the Cellulose-SB with mobile phase CO_2/2-PrOH (80/20, *v/v*), while the enantiomers of *syn*-**5a** and *syn*-**5d** were not resolved with the same

mobile phase. No chiral resolution of hydantoin *syn-***5c** was observed on this column with either MeOH, EtOH or 2-PrOH as modifiers. As seen from Table 2, compounds *syn-* and *anti-***5g** with 3-chloro-4-methylphenyl substituent at the N3 position of the hydantoin ring were always longer retained than other analytes, which implied that the interactions between these two analytes and CSP were the strongest. On the contrary, lower retention of compounds *syn-* and *anti-***5a**, *syn-* and *anti-***5b**, and *syn-* and *anti-***5c** was the result of their weaker interaction with CSP. As can be seen by comparing the results in Table 2, the retention factors of all *syn-*hydantoins were higher than *anti-*hydantoins with all three modifiers. Obviously, when branched alcohol, 2-PrOH, was used as the alcohol modifier, the retention time of most compounds was longer than that of using linear alcohols, which indicated that the steric effect of the modifier likely contributed to the decreased strengths of the interactions between the mobile phase and the CSP, resulting in the reduced elution ability of the mobile phase. The Cellulose-SB column in SFC mode exhibited better enantioseparation toward *anti-*hydantoins compared to *syn-*hydantoins. As shown in Figure 8, higher separation and resolution of the compound *anti-***5a** with allyl substituent at the N3 position of the hydantoin ring was achieved using the mobile phase CO_2/alcohol (80/20, *v/v*).
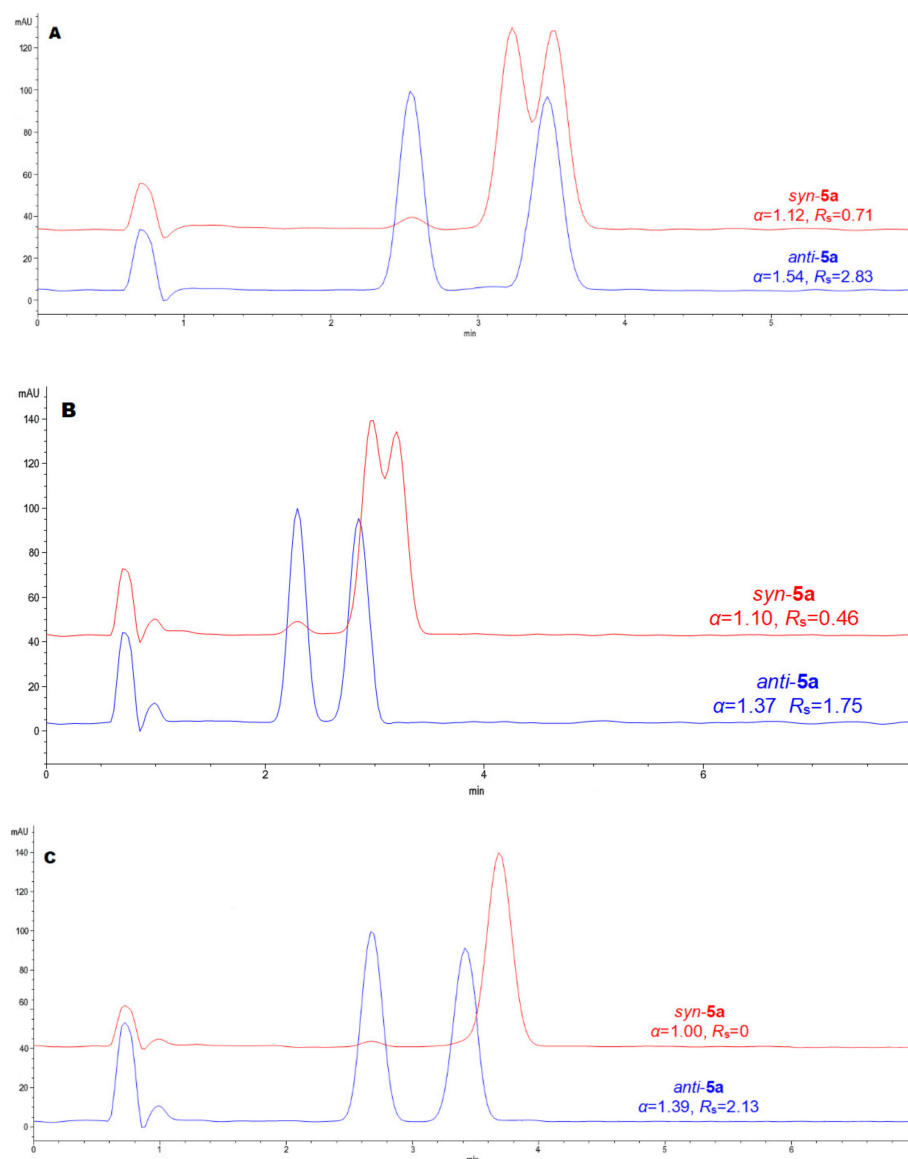

Figure 8. SFC overlay chromatograms of (±)-*syn-***5a** and (±)-*anti-***5a** on Cellulose-SB column with: (**A**) CO_2/MeOH (80/20, *v/v*), (**B**) CO_2/EtOH (80/20, *v/v*) and (**C**) CO_2/2-PrOH(80/20, *v/v*) as mobile phases.

3.3. Enantioseparation on Cellulose-SC

The results of the enantioseparations using the Cellulose-SC column in the normal and non-standard phase HPLC mode and SFC mode are summarized in Table 3.

Table 3. Chromatographic parameters for the enantioselective separations of racemic *syn*-and *anti*-3,5-disubstituted hydantoins on Cellulose-SC.

Compound	Condition *	k_1	k_2	α	R_s	Compound	Condition *	k_1	k_2	α	R_s
syn-**5a**	A	5.22	5.76	1.10	0.47	*anti*-**5a**	A	3.07	6.97	2.27	4.44
	B	0.06	0.06	1.00	-		B	0.11	0.11	1.00	-
	C	0.96	0.96	1.00	-		C	0.79	0.79	1.00	-
	D	0.76	0.76	1.00	-		D	0.68	0.68	1.00	-
	E	1.13	1.37	1.21	0.27		E	0.87	2.05	2.36	2.26
syn-**5b**	A	3.39	3.96	1.17	0.80	*anti*-**5b**	A	2.03	4.70	2.32	4.38
	B	0.07	0.07	1.00	-		B	0.12	0.12	1.00	-
	C	1.03	1.03	1.00	-		C	0.83	0.83	1.0	-
	D	0.80	0.80	1.00	-		D	0.70	0.70	1.00	-
	E	1.20	1.61	1.34	0.80		E	0.97	2.37	2.44	2.47
syn-**5c**	A	2.54	3.79	1.49	2.10	*anti*-**5c**	A	1.53	2.24	1.46	-
	B	0.07	0.07	1.00	-		B	0.14	0.14	1.00	-
	C	1.02	1.49	1.46	1.14		C	0.80	1.03	1.29	0.52
	D	0.77	1.07	1.39	0.66		D	0.62	0.79	1.27	0.52
	E	1.24	1.53	1.23	0.48		E	0.85	1.22	1.44	0.77
syn-**5d**	A	8.51	9.61	1.13	0.68	*anti*-**5d**	A	5.09	13.57	2.67	5.27
	B	0.05	0.05	1.00	-		B	0.10	0.10	1.00	-
	C	1.38	1.38	1.00	-		C	1.20	1.20	1.00	-
	D	1.06	1.06	1.00	-		D	0.93	1.08	1.16	-
	E	1.62	2.02	1.25	0.70		E	1.35	3.51	2.60	3.41
syn-**5e**	A	6.19	6.19	1.00	-	*anti*-**5e**	A	3.80	6.22	1.64	2.61
	B	0.06	0.06	1.00	-		B	0.11	0.11	1.00	-
	C	1.79	1.79	1.00	-		C	1.50	1.50	1.00	-
	D	1.28	1.28	1.00	-		D	1.11	1.11	1.00	-
	E	2.03	2.03	1.00	-		E	1.63	2.73	1.67	1.92
syn-**5f**	A	8.91	8.91	1.00	-	*anti*-**5f**	A	6.52	13.81	2.12	3.29
	B	0.05	0.05	1.00	-		B	0.09	0.09	1.00	-
	C	2.14	2.14	1.00	-		C	1.74	1.74	1.00	-
	D	1.77	2.37	1.34	1.14		D	1.55	1.55	1.00	-
	E	3.13	9.66	3.08	5.38		E	3.00	6.65	2.22	3.55
syn-**5g**	A	13.49	33.60	2.49	5.00	*anti*-**5g**	A	11.02	23.05	2.09	3.99
	B	0.07	0.07	1.00	-		B	0.13	0.13	1.00	-
	C	2.91	2.91	1.00	-		C	2.01	2.54	1.26	0.98
	D	2.41	3.15	1.31	1.22		D	2.15	2.15	1.00	-
	E	4.77	12.01	2.52	4.86		E	5.01	9.30	1.86	3.32

Table 3. *Cont.*

Compound	Condition *	k_1	k_2	α	R_s	Compound	Condition *	k_1	k_2	α	R_s
	A	12.55	12.55	1.00	-		A	13.80	13.80	1.00	-
	B	0.09	0.09	1.00	-		B	0.13	0.16	1.23	-
syn-**5h**	C	2.30	3.40	1.48	1.87	*anti*-**5h**	C	2.22	2.22	1.00	-
	D	1.98	4.66	2.35	3.96		D	2.03	2.86	1.41	1.24
	E	4.77	12.01	2.52	4.86		E	5.18	17.36	3.35	6.58
	A	4.66	7.23	1.55	2.17		A	3.88	3.88	1.00	-
	B	0.04	0.04	1.00	-		B	0.09	0.09	1.00	-
syn-**5i**	C	1.34	1.92	1.43	1.27	*anti*-**5i**	C	1.26	1.26	1.00	-
	D	0.94	1.48	1.57	1.27		D	0.89	0.89	1.00	-
	E	1.53	2.34	1.53	1.53		E	1.44	1.44	1.00	-

* Chromatographic conditions: mobile phase, A, *n*-hexane/2-PrOH (90/10, *v/v*), flow rate 1 mL min^{-1}; B, 100% DMC, flow rate 1 mL min^{-1}; C, CO_2/MeOH (80/20, *v/v*), flow rate 4 mL min^{-1}, backpressure 15 MPa; D, CO_2/EtOH (80/20, *v/v*), 4 mL min^{-1}, backpressure 15 MPa; **E**, CO_2/2-PrOH (80/20, *v/v*), flow rate 4 mL min^{-1}, backpressure 15 MPa. Detection wavelength in each condition was 254 nm. Column temperature of condition A and B is 30 °C, of C, D and E is 35 °C. The chromatographic parameters k_1, k_2, α and R_s are defined in Section 2.

When *n*-hexane/2-PrOH (90/10, *v/v*) was used as the mobile phase, the retention factors of the first-eluting enantiomers of compounds *syn*- and *anti*-**5g** and **5h** were higher than of other hydantoins. This implies that the interactions between these analytes and CSP were the strongest. A possible reason may be the presence of two groups at the *meta*-position of the phenyl ring attached to the N3 position of these hydantoins. On the contrary, the lower retention of compounds *anti*-**5b**, *syn*-**5c** and *anti*-**5c** was the result of their weaker interaction with CSP, possibly due to an alkyl or cycloalkyl substituent at the N3 position of the hydantoin ring. The longer retention was not evidently always accompanied with better enantioseparation. Among all eighteen analytes, baseline separations of nine pairs of enantiomers were achieved using this mobile phase system. It is interesting to notice that the Cellulose-SC column did not show chiral recognition ability toward any of the *syn*- and *anti*-hydantoin racemates with DMC as the mobile phase. An explanation for this possible supramolecular effect could be the same as for the Cellulose-SB column. The HPLC mobile phase composition was found to influence the retention time and resolution of the analyzed hydantoin enantiomers. The effects of *n*-hexane/2-PrOH (90/10, *v/v*) versus DMC on enantioselectivity of allyl hydantoins *syn*-**5a** and *anti*-**5a** using the Cellulose-SC column are shown in Figure 9. The enantiomers of *anti*-**5a** were well separated (R_s = 4.44), while the enantiomers of its diastereoisomer *syn*-**5a** were only partially separated (R_s = 0.47) under the normal phase HPLC mode. No chiral recognition was observed for both allyl hydantoins *syn*-**5a** and *anti*-**5a** under DMC mobile phase.

The Cellulose-SC column did not exhibit an enantiorecognition ability for most of the tested racemates using CO_2/MeOH (80/20, *v/v*). For compounds *syn*-**5c**, *anti*-**5c**, *anti*-**5g** and *syn*-**5i**, only a partial enantioseparation was achieved. However, baseline separation was achieved for only one hydantoin, *syn*-**5h**, with 3,5-dimethylphenyl group at the N3 position of the hydantoin ring when MeOH was selected as a modifier. When 2-PrOH was used as the alcoholic modifier, eleven hydantoin racemates were baseline separated. The compounds *syn*-**5a-d** and *anti*-**5c** attained partial separation, while enantiomers of compounds *syn*-**5e** and *anti*-**5i** were not separated. When EtOH was used, six compounds attained partial separation and only compound *syn*-**5h** was separated to baseline. Moreover, when using 2-PrOH α, values were larger than those obtained with EtOH as the modifier.
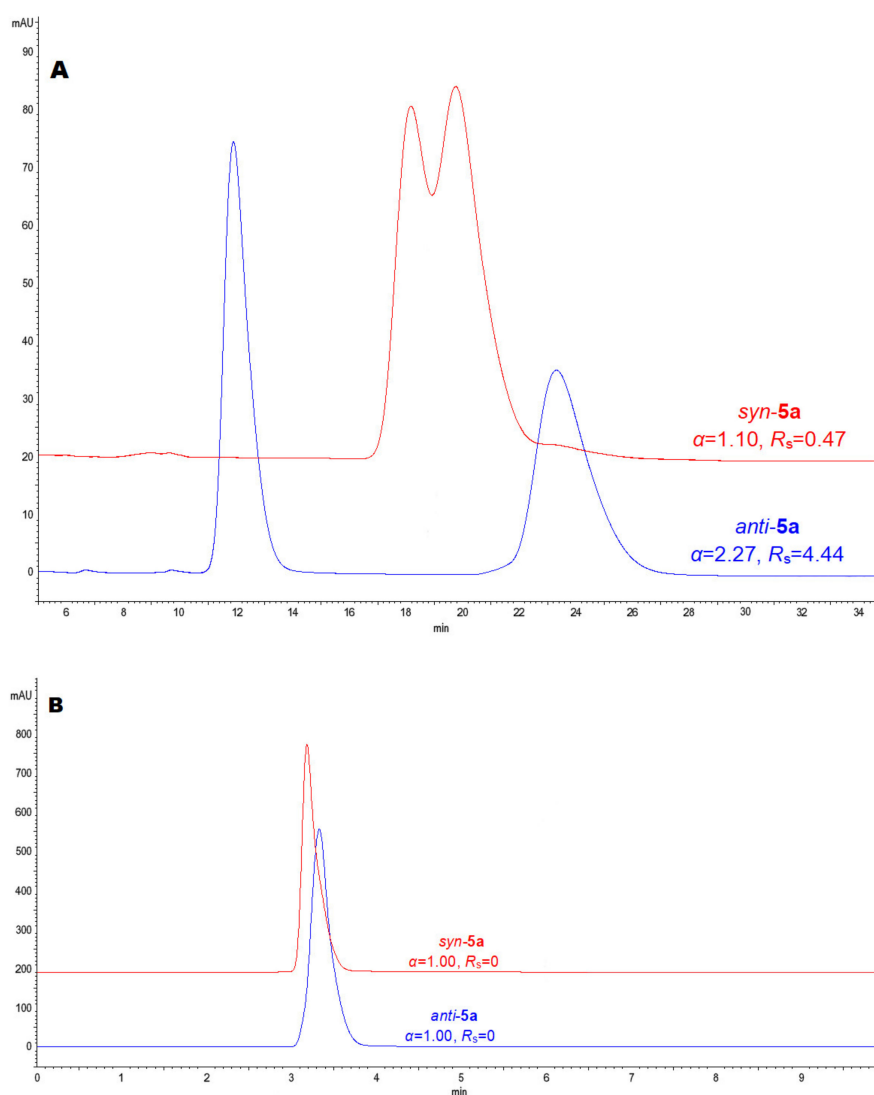
Figure 9. HPLC overlay chromatograms of (±)-*syn*-**5a** and (±)-*anti*-**5a** on Cellulose-SC column with: (**A**) *n*-hexane/2-PrOH (90/10, *v/v*) and (**B**) 100% DMC as mobile phases.

3.4. Recognition Complementarities of Three Tested Immobilized CSPs

As described in Sections 3.1–3.3, a number of baseline-separated hydantoins using three different immobilized CSPs is seventeen, sixteen, and nine for columns Amylose-SA, Cellulose-SB and Cellulose-SC, respectively, when using the *n*-hexane/2-PrOH (90/10, *v/v*) mobile phase system. Under non-standard HPLC conditions (DMC), the enantiomers of eight hydantoins were separated at baseline on the Amylose-SA column, while baseline separation of only four hydantoins was achieved on the column Cellulose-SB. No chiral resolution was observed on the Cellulose-SC with DMC as the mobile phase. Among eighteen hydantoins, baseline separations of fourteen pairs of enantiomers were achieved on the immobilized Cellulose-SB column by SFC, using the mobile phase CO_2/MeOH (80/20, *v/v*) followed by the Amylose-SA column (thirteen enantiomers of eighteen tested compounds) and the Cellulose-SC (one enantioseparation of eighteen). Operating in SFC mode, the Cellulose-SC column provided poor enantioseparations for these kinds of compounds when MeOH and EtOH were used as polar modifiers. However, when switched to 2-PrOH as the modifier, baseline separation of the eleven hydantoins was obtained on this column. Baseline separation of a great number of 3,5-disubstituted hydantoin enantiomers was achieved on the Amylose-SA and Cellulose-SB columns with CO_2/alcohol (MeOH, EtOH, 2-PrOH) as the mobile phase.

The rate of baseline separation (r.b.s.) is defined as the ratio of baseline-separated analytes to the total samples [60]. The r.b.s. values for the immobilized column Amylose-SA, Cellulose-SB and Cellulos-SC under normal phase and non-standard HPLC conditions and under SFC conditions were always higher for *anti*-hydantoins **5a–i** than for *syn*-hydantoins **5a–i**. The Cellulose-SC column exhibits quite poor performances for the series of hydantoins under investigation. Neither *syn*-hydantoins **5a–i** nor *anti*-hydantoins **5a–i** were separated on Cellulose-SC under the mobile phase DMC. Furthermore, the *anti*-hydantoins **5a–i** were not separated on this column using the mobile phase of supercritical CO_2 and the alcoholic modifiers (MeOH and EtOH). With regard to the number of baseline separations, the enantioseparation ability of the three columns decreased in the order Amylose-SA > Cellulose-SB > Cellulose-SC. Amylose-SA provided greater enantioresolution toward the majority of the tested analytes. The amylose-based CSP is considered to be more helical in nature than cellulose-derived CSP [52]. Consequently, the difference in helical structures between amylose and cellulose resulted in different enantiorecognition behaviors [61,62]. It is obvious from Table 4 that the Amylose-SA column has better chiral recognition capacities than Cellulose-SB. Furthermore, it can be seen that the Cellulose-SB column is more efficient than the Cellulose-SC column due to the presence of chlorine atoms in later chiral selector. The electronegative nature of chlorine atoms makes phenyl ring electrons deficient, and this consequently leads to poor π-π interactions and low chiral recognition capabilities.

Table 4. Enantioseparation efficiencies of the three tested immobilized CSPs.

Column/CPS	Mobile Phase Condition (*v/v*)	r.b.s. *		
		syn	*anti*	*Syn + anti*
Amylose-SA	Hex/2-PrOH = 90/10	0.89	1.00	0.94
	DMC	0.33	0.56	0.44
	CO_2/MeOH = 80/20	0.44	1.00	0.72
	CO_2/EtOH = 80/20	0.56	1.00	0.78
	CO_2/2-PrOH = 80/20	0.78	1.00	0.89
Cellulose-SB	Hex/2-PrOH = 90/10	0.78	1.00	0.89
	DMC	0	0.44	0.22
	CO_2/MeOH = 80/20	0.56	1.00	0.78
	CO_2/EtOH = 80/20	0.56	0.78	0.67
	CO_2/2-PrOH = 80/20	0.33	0.89	0.61
Cellulose SC	Hex/2-PrOH = 90/10	0.33	0.67	0.50
	DMC	0	0	0
	CO_2/MeOH = 80/20	0.11	0	0.06
	CO_2/EtOH = 80/20	0.11	0	0.06
	CO_2/2-PrOH = 80/20	0.44	0.78	0.61

* r.b.s was defined as the rate of baseline separation.

4. Conclusions

In this comprehensive study, the chiral separation of eighteen 3,5-disubstituted hydantoins **5a–i** were conducted on three immobilized polysaccharide-based CSPs (Amylose-SA, Cellulose-SB and Cellulose-SC) by HPLC under normal and non-standard mobile phase and by SFC, using carbon dioxide and different alcohol modifiers (MeOH, EtOH and 2-PrOH). The column Amylose-SA turned out to be the best in both HPLC and SFC modalities. All three CSPs showed better chiral recognition toward *anti*-3,5-disubstituted hydantoins compared to *syn*-isomers, both in HPLC and SFC modes. In the HPLC, the results were better when *n*-hexane/2-PrOH (90/10, *v/v*) was used, in terms of higher separation and resolution, but with longer analysis times. We have shown that DMC can be efficiently used as a mobile phase in chiral separation of 3,5-disubstituted hydantoins on the immobilized polysaccharide-based CSPs, especially on the Amylose-SA column. Using DMC, no chiral recognition of any *syn*-hydantoins was observed on Cellulose-SB, and all of *syn*- and

anti-hydantoins on Cellulose-SC. The columns Amylose-SA and Cellulose-SB provided fine or excellent separations for these types of compounds.

References

1. Cho, S.; Kim, S.-H.; Shin, D. Recent applications of hydantoin and thiohydantoin in medicinal chemistry. *Eur. J. Med. Chem.* **2019**, *164*, 517–545. [CrossRef] [PubMed]
2. Gawas, P.P.; Buthanapalli, R.; Veeraiah, N.; Nutalapati, V. Multifunctional hydantoins: Recent advances in optoelectronics and medicinal drugs from Academia to the chemical industry. *J. Mater. Chem. C* **2021**, *9*, 16341–16377. [CrossRef]
3. Yang, X.Y.; Su, L.; Hou, X.B.; Ding, S.Y.; Xu, W.F.; Wang, B.H.; Fang, H. High-performance liquid chromatographic enantioseparation of 3,5-disubstituted hydantoins analogs and temperature-induced reversals of elution orders on a polysaccharide-based chiral stationary phase. *J. Chrom. A* **2014**, *1355*, 291–295. [CrossRef]
4. Konnert, L.; Lamaty, F.; Martinez, J.; Colacino, E. Recent Advances in the Synthesis of Hydantoins: The State of the Art of a Valuable Scaffold. *Chem. Rev.* **2017**, *117*, 13757–13809. [CrossRef] [PubMed]
5. Kartozia, I.; Kanyonyo, M.; Happaerts, T.; Lambert, D.M.; Scriba, G.K.E.; Chankvetadze, B. Comparative HPLC enantioseparation of new chiral hydantoin derivatives on three different polysaccharide type chiral stationary phases. *J. Pharm. Biomed. Anal.* **2002**, *27*, 457–465. [CrossRef]
6. Velázquez-Macías, R.F.; Aguilar-Patiño, S.; Cortez-Betancourt, R.; Rojas-Esquivel, I.; Fonseca-Reyes, G.; Contreras-González, N. Evaluation of efficacy of buserelin plus nilutamide in Mexican Male patients with advanced prostate cancer. *Rev. Mex. Urol.* **2016**, *76*, 346–351. [CrossRef]
7. Ito, Y.; Sadar, M.D. Enzalutamide and blocking androgen receptor in advanced prostate cancer: Lessons learnt from the history of drug development of antiandrogens. *Res. Rep. Urol.* **2018**, *10*, 23–32. [CrossRef]
8. Ostrowski, J.; Kuhns, J.-E.; Lupisella, J.A.; Manfredi, M.C.; Beehler, B.C.; Krystek, S.R., Jr.; Bi, Y.; Sun, C.; Seethala, R.; Golla, R.; et al. Pharmacological and X-Ray structural characterization of a novel selective androgen receptor modulator: Potent hyperanabolic stimulation of skeletal muscle with hypostimulation of prostate in rats. *Endocrinology* **2007**, *148*, 4–12. [CrossRef]
9. Cherukuvada, S.; Babu, N.J.; Nangia, A. Nitrofurantoin–*p*-aminobenzoic acid cocrystal: Hydration stability and dissolution rate studies. *J. Pharm. Sci.* **2011**, *100*, 3233–3244. [CrossRef]
10. Kim, D.; Wang, L.; Caldwell, C.G.; Chen, P.; Finke, P.E.; Oates, B.; MacCoss, M.; Mills, S.G.; Malkowitz, L.; Gould, S.L.; et al. Discovery of human CCR5 antagonists containing hydantoins for the treatment of HIV-1 infection. *Bioorg. Med. Chem. Lett.* **2001**, *11*, 3099–3102. [CrossRef]
11. El-Barbary, A.A.; Khodair, A.I.; Pedersen, E.B.; Nielsen, C. *S*-Glucosylated hydantoins as new antiviral agents. *J. Med. Chem.* **1994**, *37*, 73–77. [CrossRef] [PubMed]
12. Verlinden, Y.; Cuconati, A.; Wimmer, E.; Rombaut, B. The antiviral compound 5-(3,4-dichlorophenyl) methylhydantoin inhibits the post-synthetic cleavages and the assembly of poliovirus in a cell-free system. *Antivir. Res.* **2000**, *48*, 61–69. [CrossRef]
13. Rajic, Z.; Zorc, B.; Raic-Malic, S.; Ester, K.; Kralj, M.; Pavelic, K.; Balzarini, J.; Clercq, E.D.; Mintas, M. Hydantoin Derivatives of L- and D-amino acids: Synthesis and evaluation of their antiviral and antitumoral activity. *Molecules* **2006**, *11*, 837–848. [CrossRef] [PubMed]

14. Marton, J.; Enisz, J.; Hosztafi, S.; Timar, T. Preparation and fungicidal activity of 5-substituted hydantoins and their 2-thio analog. *J. Agric. Food Chem.* **1993**, *41*, 148–152. [CrossRef]

15. Knabe, J.; Baldauf, J.; Ahlhem, A. Racemates and enantiomers of basic, substituted 5-phenylhydantoins, synthesis and anti-arrhythmic action. *Die Pharm.* **1997**, *52*, 912–919.

16. Matsukura, M.; Daiku, Y.; Ucda, K.; Tanaka, S.; Igarashi, T.; Minami, N. Synthesis and antiarrhythmic activity of 2,2-dialkyl-1'-(*N*-substituted aminoalkyl)-spiro-[chroman-4,4'-imidazolidine]-2',5'-diones. *Chem. Pharm. Bull.* **1992**, *40*, 1823–1827. [CrossRef]

17. Anger, T.; Madge, D.J.; Mulla, M.; Riddall, D. Medicinal chemistry of neuronal voltage-gated sodium channel blockers. *J. Med. Chem.* **2001**, *44*, 115–137. [CrossRef]

18. Somsák, L.; Kovács, L.; Tóth, M.; Ösz, E.; Szilágyi, L.; Györgydeák, Z.; Dinya, Z.; Docsa, T.; Tóth, B.; Gergely, P. Synthesis of and a comparative study on the inhibition of muscle and liver glycogen phosphorylases by epimeric pairs of D-gluco- and D-xylopyranosylidene-spiro-(thio)hydantoins and *N*-(D-Glucopyranosyl) amides. *J. Med. Chem.* **2001**, *44*, 2843–2848. [CrossRef] [PubMed]

19. Oka, M.; Matsumoto, Y.; Sugiyama, S.; Tsuruta, N.; Matsushima, M. A potent aldose reductase inhibitor, (2*S*,4*S*)-6-Fluoro-2',5'-dioxospiro[chroman-4,4'-imidazolidine]-2-carboxamide (Fidarestat): Its absolute configuration and interactions with the aldose reductase by X-ray crystallography. *J. Med. Chem.* **2000**, *43*, 2479–2483. [CrossRef]

20. Nakabayashi, M.; Regan, M.M.; Lifsey, D.; Kantoff, P.W.; Taplin, M.-E.; Sartor, O.; Oh, W.K. Efficacy of nilutamide as secondary hormonal therapy in androgen-independent prostate cancer. *BJU Int.* **2005**, *96*, 783–786. [CrossRef]

21. Kassouf, W.; Tanguay, S.; Aprikian, A.G. Nilutamide as second line hormone therapy for prostate cancer after androgen ablation fails. *J. Urol.* **2003**, *169*, 1742–1744. [CrossRef] [PubMed]

22. Struck, R.F.; Kirk, M.C.; Rice, L.S.; Suling, W.J. Isolation, synthesis and antitumor evaluation of spirohydantoin aziridine, a mutagenic metabolite of spirohydantoin mustard. *J. Med. Chem.* **1986**, *29*, 1319–1321. [CrossRef] [PubMed]

23. Foulds, G.; O'Brien, M.M.; Bianchine, J.R.; Gabbay, K.H. Kinetics of an orally absorbed aldose reductase inhibitor, sorbinil. *Clin. Pharmacol. Ther.* **1981**, *30*, 693–700. [CrossRef] [PubMed]

24. Lu, H.; Kong, D.; Wu, B.; Wang, S.; Wang, Y. Synthesis and evaluation of anti-inflammatory and antitussive activity of hydantion derivatives. *Lett. Drug Des. Discov.* **2012**, *9*, 638–642. [CrossRef]

25. Fiallo, M.M.L.; Kozlowski, H.; Garnier-Suillerot, A. Mitomycin antitumor compounds: Part 1. CD studies on their molecular structure. *Eur. J. Pharm. Sci.* **2001**, *12*, 487–494. [CrossRef]

26. Youssef, D.T.A.; Shaala, L.A.; Alshali, K.Z. Bioactive hydantoin alkaloids from the red sea marine sponge *Hemimycale arabica*. *Mar. Drugs* **2015**, *13*, 6609–6619. [CrossRef]

27. Mio, S.; Ichinose, R.; Goto, K.; Sugaai, S.; Sato, S. Synthetic studies on (+)-hydantocidin (1): A total synthesis of (+)-hydantocidin, a new herbicidal metabolite from microorganism. *Tetrahedron* **1991**, *47*, 2111–2120. [CrossRef]

28. Mio, S.; Kumagawa, Y.; Sugaai, S. Three-step synthetic pathway to fused bicyclic hydantoins involving a selenocyclization step. *Tetrahedron Lett.* **1993**, *34*, 7391–7394. [CrossRef]

29. Gregoriou, M.; Noble, M.; Watson, K.; Garman, E.; Krulle, T.; Delafuente, C.; Fleet, G.; Oikonomakos, N.; Johnson, L. The structure of a glycogen phosphorylase glucopyranose spirohydantoin complex at 1.8 Å resolution and 100 K: The role of the water structure and its contribution to binding. *Protein Sci.* **1998**, *7*, 915–927. [CrossRef]

30. Shiozaki, M. Syntheses of hydantocidin and C-2-thioxohydantocidin. *Carbohyd. Res.* **2002**, *337*, 2077–2088. [CrossRef]

31. Kalník, M.; Gabko, P.; Bella, M.; Koóš, M. The Bucherer–Bergs multicomponent synthesis of hydantoins—excellence in simplicity. *Molecules* **2021**, *26*, 4024. [CrossRef] [PubMed]

32. Uemoto, H.; Tsuda, M.; Kobayashi, J. Mukanadins A−C, New bromopyrrole alkaloids from marine sponge *Agelas nakamurai*. *J. Nat. Prod.* **1999**, *62*, 1581–1583. [CrossRef] [PubMed]

33. Jimenez, C.; Crews, P. Mauritamide A and accompanying oroidin alkaloids from the sponge *Agelas mauritiana*. *Tetrahedron Lett.* **1994**, *35*, 1375–1378. [CrossRef]

34. Audion, C.; Cocandeau, V.; Thomas, O.P.; Bruschini, A.; Holderith, S.; Genta-Jouve, G. Metabolome consistency: Additional Parazoanthines from the Mediterranean zoanthid *Parazoanthus axinellae*. *Metabolites* **2014**, *4*, 421–432. [CrossRef] [PubMed]

35. Cachet, N.; Genta-Jouve, G.; Regalado, E.L.; Mokrini, R.; Amade, P.; Culioli, G.; Thomas, O.P. Parazoanthines A−E, hydantoin alkaloids from the Mediterranean sea anemone *Parazoanthus axinellae*. *J. Nat. Prod.* **2009**, *72*, 1612–1615. [CrossRef]

36. Chankvetadze, B. Recent trends in preparation, investigation and application of polysaccharide-based chiral stationary phases for separation of enantiomers in high-performance liquid chromatography. *TrAC* **2020**, *122*, 115709. [CrossRef]

37. Horváth, S.; Eke, Z.; Németh, G. A protocol to replace dedication to either normal phase or polar organic mode for chiral stationary phases containing amylose tris (3,5-dimethylphenylcarbamate). *J. Chrom. A* **2022**, *1673*, 463052. [CrossRef]

38. Yamamoto, C.; Okamoto, Y. Optically Active Polymers for Chiral Separation. *Bull. Chem. Soc. Jpn.* **2004**, *77*, 227–257. [CrossRef]

39. Foroughbakhshfasaei, M.; Dobó, M.; Boda, F.; Szabó, Z.-I.; Tóth, G. Comparative Chiral Separation of Thalidomide Class of Drugs Using Polysaccharide-Type Stationary Phases with Emphasis on Elution Order and Hysteresis in Polar Organic Mode. *Molecules* **2022**, *27*, 111. [CrossRef]

40. Cirilli, R.; Ferretti, R.; Gallinella, B.; De Santis, E.; Zanitti, L.; La Torre, F. High-performance liquid chromatography enantiosepa-ration of proton pump inhibitors using the immobilized amylose-based Chiralpak IA chiral stationary phase in normal-phase, polar organic and reversed-phase conditions. *J. Chrom. A* **2008**, *1177*, 105–113. [CrossRef]

41. Peluso, P.; Mamane, V.; Dallocchio, R.; Dessi, A.; Cossu, S. Noncovalent interactions in high-performance liquid chromatography enantioseparations on polysaccharide-based chiral selectors. *J. Chrom. A.* **2020**, *1623*, 461202. [CrossRef] [PubMed]

42. De Klerck, K.; Mangelings, D.; Heyden, Y.V. Supercritical fluid chromatography for the enantioseparation of pharmaceuticals. *J. Pharm. Biomed. Anal.* **2012**, *69*, 77–92. [CrossRef] [PubMed]

43. Bajtai, A.; Ilisz, I.; Berkecz, R.; Fülöp, F.; Lindner, W. Polysaccharide-based chiral stationary phases as efficient tools for diastereo- and enantioseparation of natural and synthetic *Cinchona* alkaloid analogs. *J. Pharm. Biomed. Anal.* **2021**, *193*, 113724. [CrossRef] [PubMed]

44. Tundo, P.; Selva, M. The Chemistry of Dimethyl Carbonate. *Acc. Chem. Res.* **2002**, *35*, 706–716. [CrossRef] [PubMed]

45. Ono, Y. Catalysis in the production and reactions of dimethyl carbonate, an environmentally benign building block. *Appl. Catal. A Gen.* **1997**, *155*, 133–166. [CrossRef]

46. Kim, K.H.; Lee, E.Y. Environmentally-benign dimethyl carbonate-mediated production of chemicals and biofuels from renewable bio-oil. *Energies* **2017**, *10*, 1790. [CrossRef]

47. Arico, F.; Tundo, P. Dimethyl carbonate: A modern green reagent and solvent. *Russ. Chem. Rev.* **2010**, *79*, 479–489. [CrossRef]

48. Tundo, P. New developments in dimethyl carbonate chemistry. *Pure Appl. Chem.* **2001**, *73*, 1117–1124. [CrossRef]

49. Abdalla, A.O.G.; Liu, D. Dimethyl carbonate as a promising oxygenated fuel for combustion: A review. *Energies* **2018**, *11*, 1552. [CrossRef]

50. Nomanbhay, S.; Ong, M.Y.; Chew, K.; Show, P.-L.; Lam, M.K.; Chen, W.-H. Organic carbonate production utilizing crude glycerol derived as by-product of biodiesel production: A Review. *Energies* **2020**, *13*, 1483. [CrossRef]

51. Lajin, B.; Goessler, W. Introducing dimethyl carbonate as a new eluent in HPLC-ICPMS: Stronger elution with less carbon. *J. Anal. At. Spectrom.* **2021**, *36*, 1272–1279. [CrossRef]

52. Armarego, W.L.F. *Purification of Laboratory Chemicals*, 8th ed.; Butterworth Heinemann: Oxford, UK, 2017; p. 31.

53. Jurin, M.; Kontrec, D.; Dražić, T.; Roje, M. Enantioseparation of (±)-trans-β-lactam Ureas by Supercritical Fluid Chromatography. *Croat. Chem. Acta* **2020**, *93*, 203–213. [CrossRef]

54. Bandyopadhyay, D.; Cruz, J.; Banik, B.K. Novel synthesis of 3-pyrrole substituted β-lactams via microwave-induced bismuth nitrate-catalyzed reaction. *Tetrahedron* **2012**, *68*, 10686–10695. [CrossRef]

55. Radolović, K.; Habuš, I.; Kralj, B. New thiazolidinone and triazinethione conjugates derived from amino-β-lactams. *Heterocycles* **2009**, *78*, 1729–1759. [CrossRef]

56. Mehra, V.; Kumar, V. Facile diastereoselective synthesis of functionally enriched hydantoins via base-promoted intramolecular amidolysis of C-3 functionalized azetidin-2-ones. *Tetrahedron Lett.* **2013**, *54*, 6041–6044. [CrossRef]

57. Ghanem, A.; Wang, C. Enantioselective separation of racemates using CHIRALPAK IG amylose-based chiral stationary phase under normal standard, non-standard and reversed phase high performance liquid chromatography. *J. Chrom. A* **2018**, *1532*, 89–97. [CrossRef]

58. Ikai, T.; Yamamoto, C.; Kamigaito, M.; Okamoto, Y. Immobilized polysaccharide derivatives: Chiral packing materials for efficient HPLC resolution. *Chem. Rec.* **2007**, *7*, 91–103. [CrossRef]

59. Zhu, B.; Zhao, F.; Yu, J.; Wang, Z.; Song, Y.; Li, Q. Chiral separation and a molecular modeling study of eight azole antifungals on the cellulose *tris* (3,5-dichlorophenylcarbamate) chiral stationary phase. *New J. Chem.* **2018**, *42*, 13421–13429. [CrossRef]

60. Pelusoa, P.; Mashiko, V.; Aubert, E.; Cossu, S. High-performance liquid chromatography enantioseparation of atropisomeric 4,4′-bipyridines on polysaccharide-type chiral stationary phases: Impact of substituents and electronic properties. *J. Chrom. A* **2012**, *1251*, 91–100. [CrossRef]

61. Okamoto, Y. Chiral polymers for resolution of enantiomers. *J. Polym. Sci. Polym. Chem.* **2009**, *47*, 1731–1739. [CrossRef]

62. Yang, G.S.; Zhan, C.Y.; Fu, G.H.; Vazquez, P.P.; Frenich, A.G.; Vidal, J.L.M.; Aboul-Enein, H.Y. Chiral separation of organic phosphonate compounds on polysaccharide-based chiral stationary phases. *Chromatographia* **2004**, *59*, 631–635. [CrossRef]